Publications of the Korean Astronomical Society
30: 389 ∼ 392, 2015 September

pISSN: 1225-1534
eISSN: 2287-6936
http://dx.doi.org/10.5303/PKAS.2015.30.2.389

DISCOVERY OF A STRONG LENSING GALAXY EMBEDDED IN A CLUSTER AT $z = 1.62$

Kenneth C. Wong[1,9], Kim-Vy H. Tran[2], Sherry H. Suyu[1], Ivelina G. Momcheva[3], Gabriel B. Brammer[4], Mark Brodwin[5], Anthony H. Gonzalez[6], Aleksi Halkola[1], Glenn G. Kacprzak[7,10], Anton M. Koekemoer[4], Casey J. Papovich[2], and Gregory H. Rudnick[8]

[1]Institute of Astronomy and Astrophysics, Academia Sinica (ASIAA), P.O. Box 23-141, Taipei 10617, Taiwan
[2]George P. and Cynthia W. Mitchell Institute for Fundamental Physics and Astronomy, Department of Physics & Astronomy, Texas A&M University, College Station, TX 77843, USA
[3]Astronomy Department, Yale University, New Haven, CT 06511, USA
[4]Space Telescope Science Institute, 3700 San Martin Drive, Baltimore, MD 21218, USA
[5]Department of Physics and Astronomy, University of Missouri, 5110 Rockhill Road, Kansas City, MO 64110, USA
[6]Department of Astronomy, University of Florida, Gainesville, FL 32611, USA
[7]Swinburne University of Technology, Victoria 3122, Australia
[8]Department of Physics and Astronomy, The University of Kansas, Malott room 1082, 1251 Wescoe Hall Drive, Lawrence, KS 66045
[9]EACOA Fellow
[10]Australian Research Council Super Science Fellow

E-mail: kcwong@asiaa.sinica.edu.tw
(Received November 30, 2014; Reviced May 31, 2015; Aaccepted June 30, 2015)

ABSTRACT

We identify a strong lensing galaxy in the cluster IRC 0218 that is spectroscopically confirmed to be at $z = 1.62$, making it the highest-redshift strong lens galaxy known. The lens is one of the two brightest cluster galaxies and lenses a background source galaxy into an arc and a counterimage. With *Hubble Space Telescope* (*HST*) grism and Keck/LRIS spectroscopy, we measure the source redshift to be $z_{\rm S} = 2.26$. Using *HST* imaging, we model the lens mass distribution with an elliptical power-law profile and account for the effects of the cluster halo and nearby galaxies. The Einstein radius is $\theta_{\rm E} = 0.38^{+0.02}_{-0.01}{}''$ ($3.2^{+0.2}_{-0.1}$ kpc) and the total enclosed mass is $\rm M_{tot}(< \theta_E) = 1.8^{+0.2}_{-0.1} \times 10^{11}\ M_\odot$. We estimate that the cluster environment contributes $\sim 10\%$ of this total mass. Assuming a Chabrier IMF, the dark matter fraction within $\theta_{\rm E}$ is $f_{\rm DM}^{\rm Chab} = 0.3^{+0.1}_{-0.3}$, while a Salpeter IMF is marginally inconsistent with the enclosed mass ($f_{\rm DM}^{\rm Salp} = -0.3^{+0.2}_{-0.5}$).

Key words: galaxies: clusters: individual (XMM-LSS02182−05102) — galaxies: elliptical and lenticular, cD — galaxies: structure — gravitational lensing: strong

1. INTRODUCTION

Gravitational lensing is a powerful tool for studying the mass structure of galaxies. Studies of early-type galaxies (ETGs) at $z < 1$ have produced interesting results on their properties. Their mass density profile slope γ' (where $\rho(r) \propto r^{-\gamma'}$) depends solely on the surface stellar mass density at fixed redshift, whereas γ' of individual galaxies does not evolve significantly. ETGs also favor a heavier stellar initial mass function (IMF). Nonetheless, the evolution of the mass distribution of ETGs at $z > 1$ is not well-constrained. Identifying strong lensing galaxies at $z > 1$ provides leverage on how ETGs assemble and tests the current cosmological paradigm.

However, strong lensing galaxies are increasingly rare at higher redshifts due to the evolving galaxy mass function, decreasing background volume, and decreasing lensing efficiency. Distant lenses also require high-resolution imaging to separate the source and lensing galaxy, and near-IR spectroscopy to confirm their redshifts. van der Wel et al. (2013) reported the most distant strong lensing galaxy known thus far at $z_{\rm L} = 1.53$ and estimated one $z_{\rm L} > 1$ system per ~ 200 arcmin^2.

Here, we report the discovery of a strong lensing galaxy embedded in a cluster at $z = 1.62$ making it the highest-redshift strong lens galaxy known (Wong et al., 2014). The system is unusual because of the high lens redshift, and the lens being the most massive cluster member. The system lies in the UDS legacy field, which has extensive multi-wavelength observations. Spectroscopy confirms the source redshift of $z_{\rm S} = 2.26$. We combine the datasets to model the lens, including its environment.

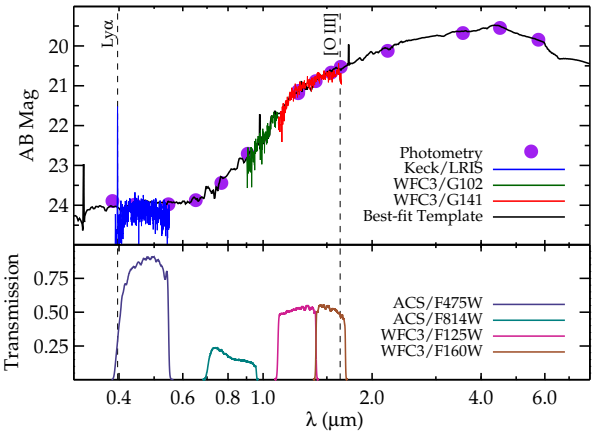

Figure 1. **Top:** Total fluxes for the lens system as measured by 3D-HST (object #31684; Skelton et al., 2014) that combines ground-based imaging with *HST* and *Spitzer* observations (purple). The best-fit SED from EAZY is included (black). Also shown are the blended Keck/LRIS spectrum (blue) and the *HST*/WFC3 G102 (green) and G141 (red) grism spectra for the lens. The spectra are arbitrarily normalized for clarity. The grism spectra trace the lens galaxy's Balmer break at $z = 1.62$. The spectra show strong Lyα and [O III] $\lambda\lambda 4959, 5007$ emission from the source at $z_S = 2.26$. **Bottom:** Filter transmission curves for the *HST* imaging used in the lens modeling. A bright point source corresponding to emission at $z_S = 2.26$ is visible in the ACS/F475 (Lyα) and WFC3/F160 ([O III] $\lambda\lambda 4959, 5007$) images.

2. OBSERVATIONS

Using Keck/LRIS, we carried out a spectroscopic survey of the cluster IRC 0218. We use the 600/4000 grism for the blue side and the 600/10000 grating for the red side of LRIS. The wavelength coverage of the extracted spectra is $3800-5800$ Å (blue side) and $7000-10000$ Å (red side). We measure a redshift for the blended spectrum composed of the lens galaxy and the lensed source. The strong emission detected at 3957 Å (Figure 1, top) has the asymmetric profile characteristic of Lyα and corresponds to a redshift of $z_S = 2.26$.

The UDS cluster falls in a legacy field that has extensive multi-wavelength observations, including deep *HST* imaging from CANDELS (0.06″/pixel; Grogin et al., 2011; Koekemoer et al., 2011) and G141 spectroscopy from 3D-HST (Brammer et al., 2012). Additional *HST* imaging and G102 spectroscopy were obtained in GO-12590 (PI: C. Papovich). Figure 1 shows the total fluxes measured for the more massive of the two brightest cluster galaxies (BCG) from the 3D-HST catalog of the UDS field (Skelton et al., 2014), which includes *Spitzer*/IRAC. The BCG shows excess flux at $\lambda < 5000$ Å due to emission from the lensed source. At longer wavelengths, the lens galaxy dominates. Grism spectroscopy confirms the BCG redshift of $z = 1.62$.

The lens and source are blended in ground-based observations, but *HST*'s resolution (Figure 2) separates the system into the BCG, an arc (object A), and a counterimage (object B). In the grism spectra, the BCG shows strong continuum. Approximately 0.5″ above the BCG

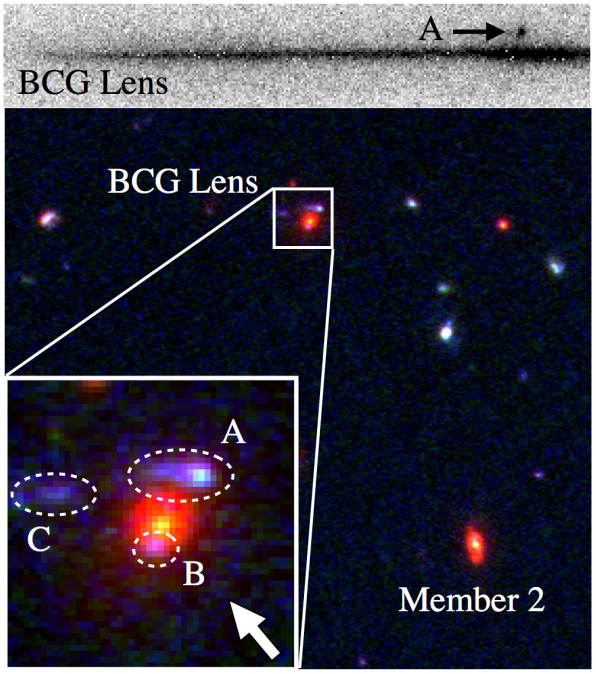

Figure 2. **Top:** Negative image of the *HST* WFC3/G141 grism spectrum for the lensing galaxy. Approximately $\sim 0.5''$ above the lens is [O III] $\lambda\lambda 4959, 5007$ emission from object A at $z_S = 2.26$. **Bottom:** False-color image of the UDS cluster core generated with *HST* imaging (ACS/F475W, ACS/F814W, WFC3/F125W, and WFC3/F160W). North and East are up and left, respectively. Labeled are the BCG lens and the other BCG (Member 2). The inset ($3'' \times 3''$) shows the lens with the arc (A) and counterimage (B) labeled. Another faint galaxy (C) is weakly detected by the grism and consistent with $z \sim 2.26$. The arrow indicates the dispersion direction of the grism observations (top).

in the G141 spectrum is a compact emission line corresponding to [O III] $\lambda\lambda 4959, 5007$ at $z_S = 2.26$ from object A. We also detect [O III] $\lambda\lambda 4959, 5007$ corresponding to object B once we remove the lens galaxy's light. The faint object C shows weak [O III] $\lambda\lambda 4959, 5007$ in the grism spectrum consistent with a redshift of $z_S = 2.26$.

3. MODELING THE STRONG LENSING SYSTEM

Combining our Keck spectroscopy and *HST* observations, we confirm that the strong lensing system is composed of the BCG lens and source. We model the system with the Glee software (Suyu & Halkola, 2010). Lensing mass distributions are parametrized profiles, and background sources are modeled on a pixel grid. The lens galaxy light distributions are modeled as Sérsic profiles. Unresolved point sources on the pixel grid are modeled as point images on the image plane. Model parameters of the lens and the source are constrained through Markov Chain Monte Carlo (MCMC) sampling.

Taking a 27×27 pixel region around the lens, we utilize the deepest *HST* images spanning the widest wavelength range: ACS/F475W, ACS/F814W, WFC3/F125W, and WFC3/F160W (Figure 3, top rows). We model the lens galaxy as an elliptical singular power-law mass distribution with a uniform prior

on the mass profile slope. The projected axis ratio has a uniform prior with the position angle as a free parameter. The normalization of the mass profile is set by the Einstein radius $\theta_{\rm E}$, which is also a free parameter. We adopt a Gaussian prior on the mass centroid with a width of $\sigma = 0.05''$ that is centered on the fitted light centroid of the lens galaxy in the WFC3/F160W image ($\lambda_{\rm rest} \sim 0.6$ μm).

We first remove the lens galaxy's light using a Sérsic profile. In F814W, we exclude the annular region containing the lensed images (objects A & B; Figure 2) when fitting the lens light profile. Because the lens is considerably brighter than the counterimage (object B; Figure 2) in F125W and F160W, we exclude only the half-annulus around arc A in these two bands.

To constrain the lens mass parameters, we use pixels in the annular regions in F475W and F814W and the half-annular regions in F125W and F160W (Figure 3, second row) containing the lensed images. GLEE simultaneously models across the four bands and reconstructs the source onto a grid of 20×20 pixels with a resolution of $\sim 0.05''$. Our lens model requires a point source convolved with the point-spread function (PSF) coincident with the peak surface brightness in image A (Figure 2). The position of this point source linked across all filters and fit simultaneously with the lens mass parameters. The counterimage of the point source is not modeled separately given its low magnification.

The lens galaxy is embedded in a cluster, and the overdense environment may affect the lens model (e.g., Wong et al., 2011). We model cluster galaxies within $2'$ of the lens as singular isothermal spheres truncated at r_{200} and estimate their virial masses from their stellar masses. We parameterize the cluster's dark matter halo as a spherical NFW profile with a mass of 7.7×10^{13} $M_\odot$ centered at the peak of the X-ray emission (source 12A in Pierre et al., 2012).

4. RESULTS

With our fiducial lens model, we measure an Einstein radius of $\theta_{\rm E} = 0.38^{+0.02}_{-0.01}''$ ($3.2^{+0.2}_{-0.1}$ kpc) and total mass enclosed within $\theta_{\rm E}$ of $1.8^{+0.2}_{-0.1} \times 10^{11}$ $M_\odot$. From our environment model, we estimate that the cluster halo and other cluster members contribute $\sim 10\%$ of this enclosed mass, consistent with results at $z \lesssim 0.5$. The lens galaxy's mass within $\theta_{\rm E}$ is thus $\sim 1.6 \times 10^{11}$ $M_\odot$.

Papovich et al. (2012) measure the total stellar mass assuming a Chabrier IMF with solar metallicity. We integrate the light profile and calculate the stellar mass within $\theta_{\rm E}$ to be $1.3^{+0.5}_{-0.2} \times 10^{11}$ $M_\odot$, corresponding to a dark matter fraction of $f_{\rm DM}^{\rm Chab}(< \theta_{\rm E}) = 0.3^{+0.1}_{-0.3}$. If we use a Salpeter IMF, which seems to be preferred for ETGs at $z < 1$, the enclosed stellar mass is $2.2^{+0.9}_{-0.4} \times 10^{11}$ $M_\odot$ and is larger than the enclosed total mass ($f_{\rm DM}^{\rm Salp}(< \theta_{\rm E}) = -0.3^{+0.2}_{-0.5}$), albeit at marginal significance. This is an upper limit on the dark matter fraction of the galaxy, as the environment contributes $\sim 10\%$ of the total mass within $\theta_{\rm E}$.

In the three reddest filters (the lens is undetected in F475W), the centroids of the lens light profile and of the mass model are offset by as much as ~ 1.5 pixels ($\sim 0.1''$; Figure 3). The lens light centroid shifts among different bands, suggesting that the youngest stars are displaced from the older population. The different stellar populations may not all directly trace the dark matter.

There is residual image flux (Figure 3, fourth row) that we attribute to compact emission regions in the source. The residuals shift in both intensity and position among the bands, likely because of different emission lines (Figure 1, bottom): F814W samples only the continuum and has the smallest residuals, while F475W has Lyα and F160W has [O III] $\lambda\lambda 4959, 5007$ emission. We speculate that offset [O II] $\lambda 3727$ emission may be causing the weaker residual feature in F125W. These residuals cannot come from the same source position, as lensing is achromatic. The residuals corresponding to the emission-line regions extend in the direction of the arc (object A), i.e. tangential to the lens galaxy. This implies that the emission-line regions are elongated and/or stretched due to lensing.

Strong lensing galaxies at $z > 1$ directly measure the stellar build-up of massive galaxies (e.g., whether the IMF evolves with redshift), and their number tests the current cosmological paradigm. Ongoing and upcoming deep imaging surveys should identify more lensing candidates to directly study the dark matter and light distributions of structures when the universe was $\sim 30\%$ of its current age.

REFERENCES

Brammer, G. B., et al., 2012, 3D-HST: A Wide-field Grism Spectroscopic Survey with the Hubble Space Telescope, ApJS, 200, 13

Grogin, N. A., et al., 2011, CANDELS: The Cosmic Assembly Near-infrared Deep Extragalactic Legacy Survey, ApJS, 197, 35

Koekemoer, A. M., et al., 2011, CANDELS: The Cosmic Assembly Near-infrared Deep Extragalactic Legacy Survey—The Hubble Space Telescope Observations, Imaging Data Products, and Mosaics, ApJS, 197, 36

Papovich, C. J., et al., 2012, CANDELS Observations of the Structural Properties of Cluster Galaxies at z = 1.62, ApJ, 750, 93

Pierre, M., et al., 2012, A Chandra View of the z = 1.62 Galaxy Cluster IRC-0218A, A&A, 540, 4

Skelton, R. E., et al., 2014, 3D-HST WFC3-selected Photometric Catalogs in the Five CANDELS/3D-HST Fields: Photometry, Photometric Redshifts, and Stellar Masses, ApJS, 214, 24

Suyu, S. H. & Halkola, A., 2010, The Halos of Satellite Galaxies: the Companion of the Massive Elliptical Lens SL2S J08544-0121, A&A, 524, 94

van der Wel, A., et al., 2013, Discovery of a Quadruple Lens in CANDELS with a Record Lens Redshift z = 1.53, ApJ, 777L, 17

Wong, K. C., et al., 2011, The Effect of Environment on Shear in Strong Gravitational Lenses, ApJ, 726, 84

Wong, K. C. et al., 2014, Discovery of a Strong Lensing Galaxy Embedded in a Cluster at z = 1.62, ApJ, 789L, 31

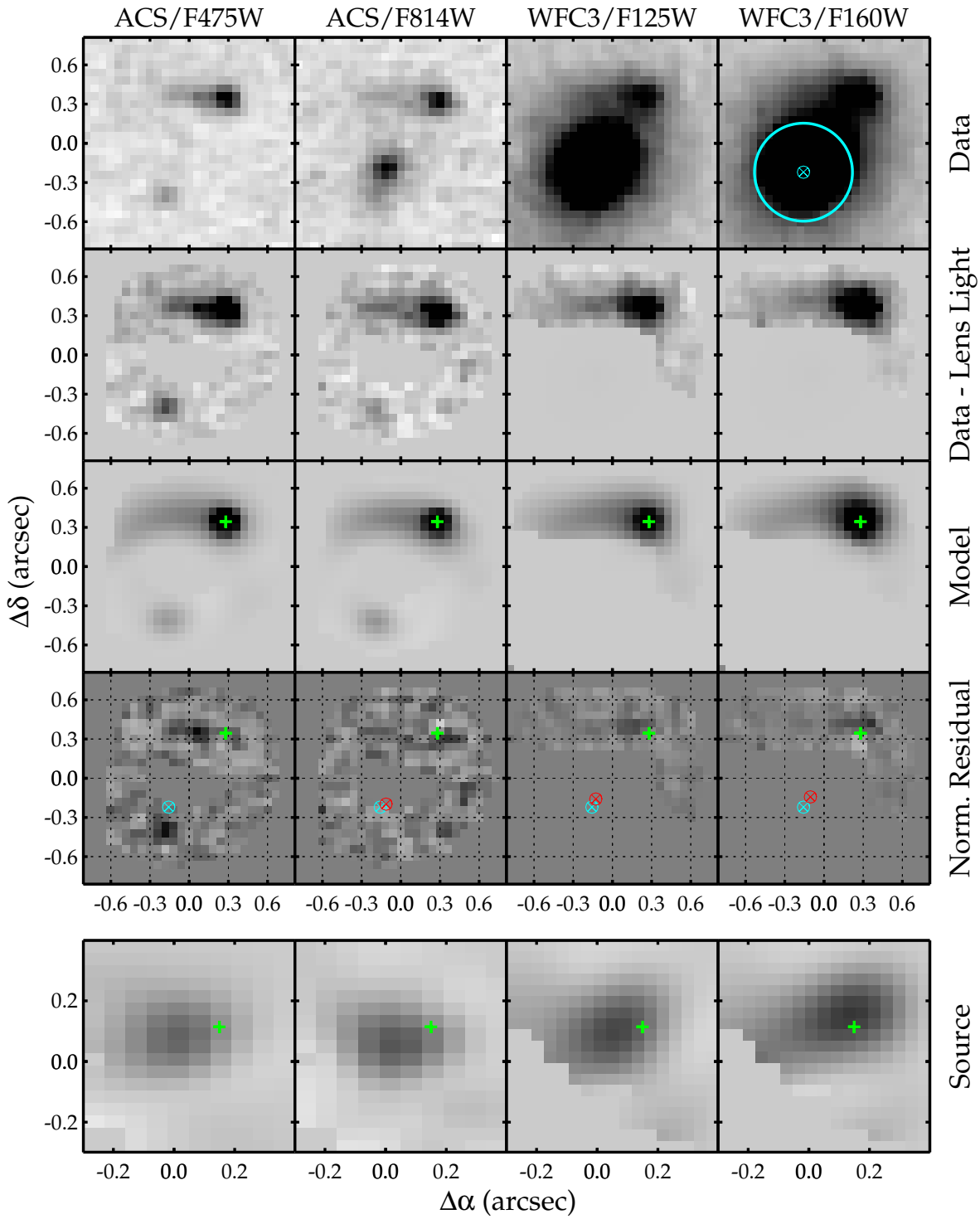

Figure 3. **Top Row:** Negative *HST* images of the strong lensing system in the ACS/F475W, ACS/F814W, WFC3/F125W, and WFC3/F160W filters. The images are $1.62''$ on a side. The cyan cross denotes the centroid of the mass distribution, and the cyan circle the Einstein radius. **Second Row**: Images with the lens light subtracted. Only the pixels containing the lensed source are shown and used in the lens modeling. **Third Row**: Reconstructed image plane from the best-fit lens model. The model includes a compact emission region (point source convolved with the PSF) marked by the green cross. **Fourth Row**: Normalized image plane residuals where the color scale shows the $\pm 2\sigma$ range. The green cross denotes the position of the compact source as in the third row. The magnification varies by ~ 0.5 over the region around the compact source. Grid lines are overplotted for clarity. The centroid of the lens light distribution in each filter (red cross) is offset from that of the mass (cyan cross). **Bottom Row**: Extended source reconstruction. The compact emission region is not reconstructed since it is unresolved, but its inferred location from the lens model is indicated (green cross). The source morphology is less constrained in the F125W and F160W because only the upper half-annulus is used in the model. The compact emission is offset from the source galaxy's center in all filters.